Combined Frequency Domain and Time Domain Airborne Data for Environmental and Engineering Challenges

Evgeny V. Karshakov[1,2], Yury G. Podmogov[1], Vladimir M. Kertsman[3] and John Moilanen[1,2]
[1]Geotechnologies LLC, 5/7 – 2 Rozhdestvenka, Moscow, Russia, 107031
Email: karshakov@geotechnologies-rus.com
[2]Trapeznikov Institute of Control Sciences of Russian Academy of Sciences, 65 Profsoyuznaya, Moscow, Russia, 117997
[3]Faculty of Geology, Lomonosov Moscow State University, 1 Leninskie Gory, Moscow Russia, 119991

ABSTRACT

We describe the main properties of the EQUATOR airborne geophysical system and how the system can be employed to solve some engineering and environmental problems. To date, the EQUATOR system has been used for groundwater search in 2014 and 2015 in Siberia. The name "EQUATOR" originates from the intention to EQUATE, or to balance time and frequency domain approaches in airborne electromagnetics, which is why the system was originally designed. To the best of our knowledge, EQUATOR is the only system to collect electromagnetic data both in time and in frequency domains. We further explain the difference between the two methods on some numerical and field examples. Also we describe some advantages of their coupling. In particular, by virtue of our approach, a numerically more robust solution of the one-dimensional electromagnetic inverse problem may be achieved. The recorded full-time measurements are further converted to in-phase, quadrature and off-time responses, as opposed to standard frequency or time domain solutions, which have been widely adapted within the industry. When inverting the data, our main focus is within the top 100 m of the Earth, which are the most relevant for engineering and environmental studies. We emphasize that a combined use of frequency and time domain data gives more detailed information about geological structures in the near-surface. As an example, we present some case studies obtained over a platform (Siberia) and a crystalline shield (Western Africa) setting. We further suggest using these results in such near-surface studies as sediment thickness estimation, soil state analysis, groundwater search, and geological structural analysis.

Introduction

High resolution ground geophysical surveys are traditionally used in engineering and environmental studies. However, the size of the area covered by ground survey is limited due to high costs and logistical limitations, especially in rough terrain and climate conditions. Airborne methods, on the other hand, are highly efficient and provide comparable quality of information. Modern airborne geophysical systems, including EQUATOR (Moilanen *et al*., 2013), measure magnetic and electromagnetic fields simultaneously and, in some cases, the Earth's surface radiation intensity. Using modern combined GPS/GLONASS technology it is possible to achieve the positioning accuracy of less than 1 m (Leick *et al*., 2015).

Precise magnetic measurements can provide a detailed distribution of magnetic susceptibility in the upper ground layers and reveal tectonic faults, high fracture areas, paleo-valleys, karst zones and other heterogeneities (Hinze *et al*., 2013). Precise electromagnetic (EM) measurements help to recover electrical resistivity distributions in the range from fractions to tens of thousands of Ohm-meters and for depths from a few to several hundred meters (Zhdanov, 2009). Lateral resolution is normally within a range from 10 to 50 m.

A description of the EQUATOR is given by Moilanen *et al*. (2013), and Volkovitsky and Karshakov (2013). Felix *et al*. (2014) provides a detailed comparison of airborne (EQUATOR) and ground (time-domain system Tsikl-5 and frequency-domain system EM34-3XL) EM data, obtained for purposes of kimberlite

 DOI: #10.2113/JEEG22.1.1

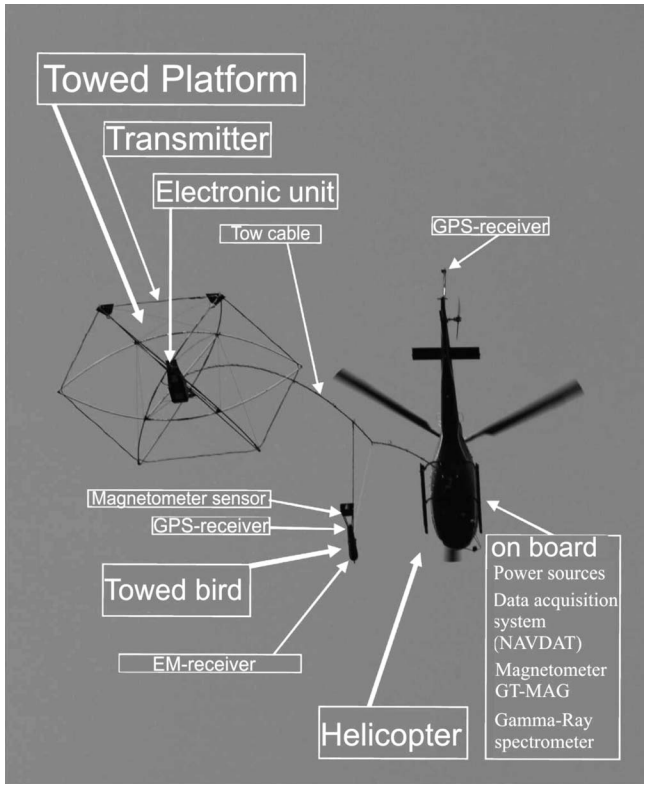

Figure 1. Airborne system EQUATOR.

exploration. Airborne and ground data showed comparable sensitivity and resolution (Fig. 2), with the airborne technology being by far superior in productivity and sampling rate.

The current paper is organized as follows: first, the basic features of the EQUATOR system are discussed, focusing on its ability to provide EM data in time and frequency domains simultaneously. We explain the difference between these two methods and the advantages of their combination. We then provide combined inversion results for a synthetic model with low electrical resistivity contrasts in upper 100 m. We further show the potential applications of EQUATOR to engineering and environmental problems, based on this modeling. Next, the EM, magnetic and altimeter data as well as geological information, which may be extracted are considered for the exercise. Lastly, we show examples of data processing results, obtained over platform (Siberia) and crystalline shield (Western Africa) environments.

System Specifications

The EQUATOR is a helicopter-borne system designed for high-precision airborne magnetic and electromagnetic measurements (Moilanen *et al*., 2013). EQUATOR includes combined time-domain (TD) and frequency-domain (FD) electromagnetics, magnetics, gamma-ray spectrometry, navigation tools, and a data acquisition system. The EM-transmitter is towed by helicopter using 70 m tow-cable (Fig. 1). The receiver bird is attached to the tow-cable 40 m away from transmitter. The transmitter is a loop of 11 m in diameter with five turns. The primary field is generated by repeated bipolar half-sine shaped pulses of 1.9 ms length. The base frequency of EQUATOR is 77 Hz. Peak dipole moment is 100,000 A·m^2. The transmitter current turn-off was made as short as possible in order to increase energy of early time channels and high frequencies. The current drops from 35% of its peak value to 0 in 90 μs, while the whole turnoff time is about 90 ms.

The three-component EM-receiver is located in a separate bird, positioned approximately 20 meters vertically and 30 meters horizontally (along flight direction) away from the transmitter. The same receiver bird carries a Scintrex CS-3 (or similar) magnetic sensor. The in-flight bird swing is accounted for using an algorithm specifically designed to determine the geometry of the system with an accuracy of 10 cm (Karshakov

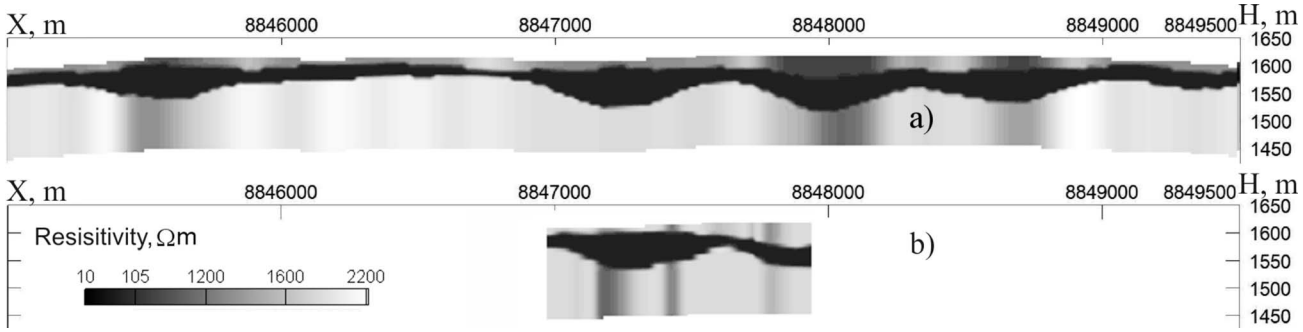

Figure 2. Comparison of resistivity sections (results of 1D inversion) based on: a) airborne EM data; b) ground EM data (Western Africa).

Table 1. Time domain channels of the EQUATOR.

Channel	Center of time gate, μs	Channel	Center of time gate, μs	Channel	Center of time gate, μs
1	2.5	6	70	11	852.5
2	7.5	7	122.5	12	1,397.5
3	15	8	197.5	13	2,265
4	27.5	9	322.5	14	3,662.5
5	45	10	525		

et al., 2013). The algorithm is based on measurements of fields of three dipoles: one main vertical dipole and two additional horizontal dipoles, mounted on the same frame. By measuring the fields of three linearly independent dipoles it is possible to calculate position of EM-receiver with respect to transmitter (Pavlov *et al*., 2010). Georeferencing is carried out using satellite navigation system GPS/GLONASS operated in differential mode (Leick *et al*., 2015). Flight altitude is monitored by a radar altimeter mounted on the transmitter.

To increase the system bandwidth a high frequency signal is added to the pulse (Volkovitsky and Karshakov, 2013). In post-processing this signal is excluded from time-domain data in order to record pure off-time decay. Such approach is possible due to the full-time measurements. The EQUATOR measures full-time mixed signal (200,000 samples per second). After the data are processed in frequency and time domains the outputs include: 1) 25 samples per second of magnetic field; 2) 6.61 samples per second of B-field and dB/dt in 14 time-gates starting from the time the current in the loop is switched off (Table 1); and 3) 6.61 samples per second of in-phase and quadrature field components at 14 most valuable frequencies of the primary signal spectrum (Table 2). The three highest frequencies in Table 2 are available due to the additional signal.

The average flight speed along the survey line is about 150 km/h (42 m/s), which converts into EQUATOR sampling rates of approximately 6 meters for EM measurements and approximately 2 meters for total magnetic intensity measurements. The cutoff frequency of the filter used in EM-receiver signal processing is about 25 kHz. The frequency response of the filter is taken into account both for apparent resistivity calculation and for solving of one-dimensional (1D) inverse problem. Therefore, the filter influence on the resistivity parameters at the early time channels is fully taken into account when processing the data.

Table 2. Frequency domain channels of the EQUATOR.

Channel	Frequency, Hz	Channel	Frequency, Hz	Channel	Frequency, Hz
15	77	20	848	25	1,774
16	231	21	1,003	26	3,163
17	385	22	1,157	27	6,250
18	540	23	1,466	28	11,959
19	694	24	1,620		

Environmental and Engineering Applications

The objectives of engineering and environmental studies often focus on the Earth's top 100 meters. EQUATOR has been successfully tested in a complicated geology with thick permafrost overlaying the confined saltwater (freshwater) aquifers. Although the survey was aimed at groundwater mapping, the described setting may constitute similarities with potential geotechnical and environmental applications. All the following examples have been chosen to illustrate the advantages of using EQUATOR for high-resolution investigations of the near-surface.

There is a known correlation between electrical conductivity of the rocks and their clay content. Clay particles are generally present in carbonaceous and terrigenous rocks. Other direct correlations between the composition of rocks and soils and their electrical properties include presence of water in the pore space and its TDS (total dissolved solids) content. Further, water content and high variability of soil resistivity can be explained by its state (frozen/thawed) and fracturing level (evolution of tectonic or karsts processes). It should be additionally noted that resistivity is one of the driving factors determining the corrosiveness of soil.

A sediment thickness map can be obtained for a large territory by virtue of 1D inversion of EM data, where structural anomalies in the upper layers can be indicated. Such large areas can be hardly covered by any ground-based method, airborne is seen as most cost-effective, notwithstanding the fact that the remote sensing technology is non-invasive and causes minimal damage to the environment.

Kozak *et al*. (2015) describes an example of combining ground (TEM-FAST 48HPC) with helicopter-borne (EQUATOR) time-domain EM methods for water exploration in severe permafrost areas (*e.g*., Yakutia, Russia). The authors emphasize that ground survey in taiga is very difficult in winter due to low temperature, but it is even more difficult in summer

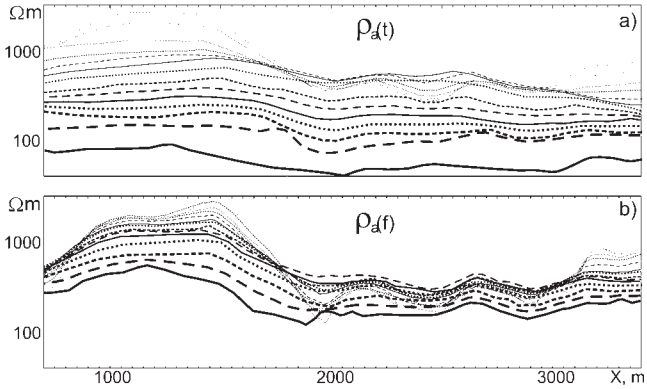

Figure 3. Apparent resistivity calculated for: a) - time domain (thick line corresponds to the time of 4.5 ms after full current cutoff, thin line - of 0.005 ms); b) - frequency domain (thick line corresponds to the frequency of 77 Hz, thin line – 11,959 Hz).

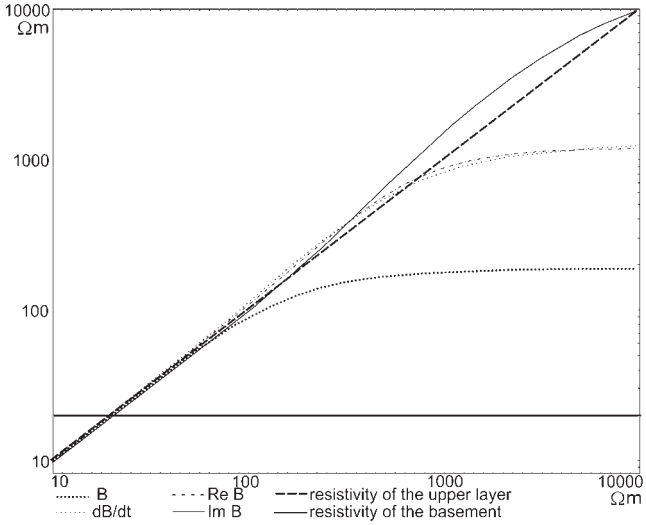

Figure 4. Dependence of apparent resistivity (vertical axis, Ω·m) on the upper layer resistivity (horizontal axis, Ω·m). Apparent resistivity was calculated for 0.005 ms time gate of B field time domain data, 0.005 ms time gate of dB/dt field time domain data, 12 kHz inphase (Re B) component frequency domain data, 12 kHz quadrature (Im B) component frequency domain data.

because of swamps, creating demand for an airborne survey. The helicopter-borne survey of the area (320 line km) was performed in two days from a remote airport (160 km from survey area). The resistivity sections based on ground and airborne data correlate well with each other, and as a result, several areas prospective for groundwater were delineated. Groundwater presence was confirmed by drilling in most of them.

Discussion of the Motivation of Combined TD and FD

Representation of EM data in both time and frequency domains is the main achievement of the EQUATOR. This became possible due to mixed form of primary field and continuous full-time measurements that allow transformation of data to the frequency domain (Volkovitsky and Karshakov, 2013). The first time full-time measurements were implemented in the transient EM system COTRAN (COrrelation of TRANsients) system in the late 1970s (Becker *et al*., 1987). Two components (XZ) receiver measured response in both on-time and off-time modes. Computer system provided data corrections for eddy currents in the aircraft fuselage (Collett, 1986). In the 1990s there were the first attempts to use processing of these data in frequency domain for elimination of various instrumentation errors (Lane *et al*., 1998). Similar processing is used in some modern systems to obtain high quality data at the earliest times of decay (Macnae and Baron-Hay, 2010).

Data processing in both frequency and time domains allows taking advantage of both representations. For example, frequency channels allow estimation of resistivity in essentially wider range than time domain channels: from fractions to tens of thousands of Ω·m (Hodges, 2013). This provides more accurate estimation of resistivity distribution in high-resistivity environments and in the upper layers and, as a consequence, more accurate mapping of geological structure in upper layers. This is crucial for solving engineering and environmental problems.

An example of apparent resistivity calculation is presented in Fig. 3, which features data processing results from survey. All graphs obtained from frequency data (Fig. 3(b)) were calculated from the quadrature response component; graphs derived from time domain data (Fig. 3(a)) were the result of the magnetic field derivative (dB/dt) processing.

To explain the difference between values of electrical resistivity calculated from different signal components the response from two-layered medium was modeled. Parameters of the model were: ρ_0 – resistivity of the top layer, $d_0 = 100$ m – thickness of the top layer, $\rho_1 = 20$ Ω·m – resistivity of the basement. The model demonstration includes changing the resistivity in the top layer, to range from 10 to 10,000 Ω·m, and the results demonstrate different sensitivity of signals in time and frequency domains. In Fig. 4 there are four graphs illustrating the dependence of apparent resistivity ρ_a on ρ_0, values of ρ_a were calculated from the B-field time domain data with a 0.025 ms time gate, dB/dt time domain data with a 0.025 ms time gate, in-phase (Re B)

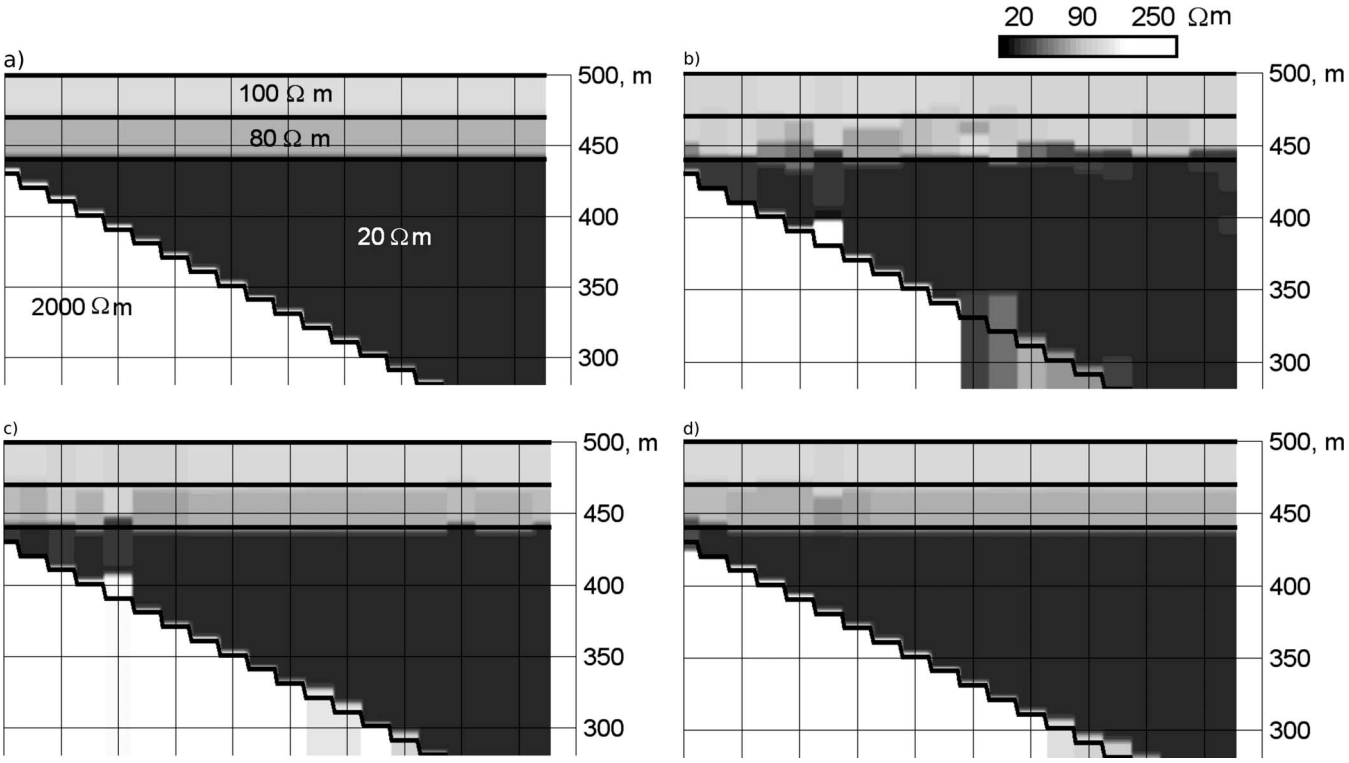

Figure 5. Results of 1D inversion based on model data: a) true model; b) inversion results for time domain; c) inversion results for frequency domain; d) combined inversion results.

component frequency domain data at 12 kHz, and quadrature (Im B) component frequency domain data at 12 kHz. It can be clearly seen that for $\rho_0 < 100$ Ω·m all apparent resistivity curves are close to each other and to ρ_0. For larger ρ_0 values, the in-phase response at the highest frequency and data in early time gates are influenced mostly by basement resistivity. As such, they become increasingly useful for engineering tasks. Apparent resistivity calculated from 0.025 ms time gate of B-field data has an asymptotic value of 200 Ω·m, in-phase component at 12 kHz and 0.025 ms time gate of dB/dt have a 1,200 Ω·m asymptote. Apparent resistivity calculated from quadrature component has almost the same sensitivity to the resistivity of the top layer, as for the entire resistivity range despite the deviation caused by conductive basement.

A similar situation is shown in the left part of Fig. 3, in which case, the highest frequency also shows high resistivity, while the latest channels' responses come from the conductive basement along the entire line. Nevertheless, the lowest frequencies, being influenced by upper resistive layer, show increased resistivity in comparison with time domain channels. At the same time, high frequencies give more detailed information about upper layers in comparison with early channels of time-domain. This fact confirms the higher efficiency of TD measurements with respect to FD in the search for deep, highly conductive targets (Kaufman, 1989). As can be seen in Fig. 4, the influence of the conductive basement is first shown in the B-field channel at 0.025 ms.

Synthetic Examples

Frequency domain information gives additional capabilities for solving inverse problems. Figure 5 shows a 1D inversion result using a four-layered model with low contrast boundary in the upper part of the section (30 m of 100 Ω·m and 30 m of 80 Ω·m). These top two layers overlay a high conductivity layer of varying thickness and 20 Ω·m resistivity. The basement is 2,000 Ω·m. The algorithm of 1D inversion is the same for time domain, frequency domain, and combined inversions. It solves for the number of layers and the resistivities starting from homogeneous half-space. The starting model for all inversions was set to a 100 Ω·m half-space. The resistivity of the basement was better recovered by time domain inversion, while the resistivity of the upper part of the section is recovered better by frequency domain inversion. Combined inversion shows good recovery of the entire model. We note that time-

domain inversion had difficulties at 6th station (Fig. 5(b)), while frequency-domain had some trouble fitting the data from station 5 (Fig. 5(c)). Combined inversion had no such difficulties at either of these two stations.

Hence, retaining all the features of TD systems, EQUATOR provides additional capabilities in the data interpretation by adding the EM information in frequency domain, which increases both the exploration and mapping effectiveness. It is worth mentioning that all the information obtained from frequency domain possibly could be extracted from time domain data. But, for this purpose, obviously, on-time data processing should be used. The choice was made in favor of frequency-domain, since this form of data representation is probably better established within the geophysical community. On-time channels are highly dependent on the shape of transmitter pulse. Also, the highest frequencies are better introduced in frequency domain due to added high frequency signal. Furthermore, from a mathematical standpoint, in some cases a local minimum in time-domain solver could be not an extremum in frequency-domain, and vice versa, as can be seen from the example provided above.

Field Examples

EM Data Processing

A detailed test survey of 1:5,000 scale, *i.e*., distance between flight lines is 50 m, with airborne system EQUATOR in Western Yakutia was aimed to estimate the exploration capabilities of the system. In addition, the results have demonstrated that the system can be effectively applied for the purpose of engineering geology. For example, resistivity maps are well correlated with rock composition (Fig. 6).

Effective algorithms of 1D inversion help to recover information about resistivity distribution not only along surface but also in depth. This allows effective estimation of depths to bedrock and lithology-petrological characteristics of rocks. Of course, there are some cases, when using simple 1D inversion is not sufficient, as in cases with complicated geologies and visible 2D and 3D effects (Ley-Cooper *et al*., 2010). More complicated inversion algorithms for EQUATOR EM-data were developed by Aarhus Geophysics (Kaminski *et al*., 2015).

Altitude Data Processing

Airborne methods use differential correction to calculate precise location of data points (Leick *et al*., 2015). This provides positioning accuracy of less than 1 meter. As a result, processing of absolute altitude and radar altimeter data allows us to obtain high detailed digital elevation model (Fig. 7). This can be further used for geomorphological analysis and to detect neo-tectonic elements of the area under study. Joint analysis of the terrain, bedrock depths and rock compositions can be useful for landslide monitoring, as well as slope stability analysis in general.

Complex Data Processing

Some results of an airborne geophysical survey at the Angolan shield in Western Africa are presented below (Felix *et al*., 2014). The survey was aimed for kimberlite exploration, but the results also provide valuable insight for engineering geology (Fig. 8). Beneath most of the study area lays ancient rocks of the crystalline shield outcrop. In some places they are covered by terrigenous sediments of Cretaceous-Quaternary age. Weathering crusts were formed on the late Archean granites and gneisses, reaching up to 70 meters in thickness. Electrical and magnetic parameters of the upper layers show a great deal of variability over the area. Apparent resistivity varies from 1 to 10,000 Ω·m within the survey area, as shown in Fig. 8(a). Frequency domain EM methods provide adequate recovery of resistivity range.

Anomalous magnetic intensity is somewhat dissected and shows amplitudes of anomalies measured in tens and hundreds of nT. Nevertheless, filtering permits detection of low-contrast local and linear anomalies of different genesis. Joint analysis of the data made it possible to carry out geological and geophysical mapping and then to investigate the structural and tectonic features of the survey area.

Contrasting geoelectrical boundaries define good depth resolution of the 1D inversion. Geoelectrical sections correlate well with the drilling results. There are three basic types of interpreted sections that include: 1) a homogeneous half-space with no sediments and only a resistive basement; 2) two-layered model with a resistive basement that is covered by conductive alluvial quaternary sediments or water-saturated weathered crusts of basement soils; and 3) a three-layered model with a resistive basement that is covered by conductive weathered crusts and highly resistive sands of Kalahari group. The western part of the survey predominantly has little sediments. The eastern part fits well with two or three layer models. Examples of geoelectrical sections are shown in Fig. 9. Profile survey data were also inverted.

The sediment thickness map is based on 1D inversion of geoelectrical cross-sections (Fig. 10). It

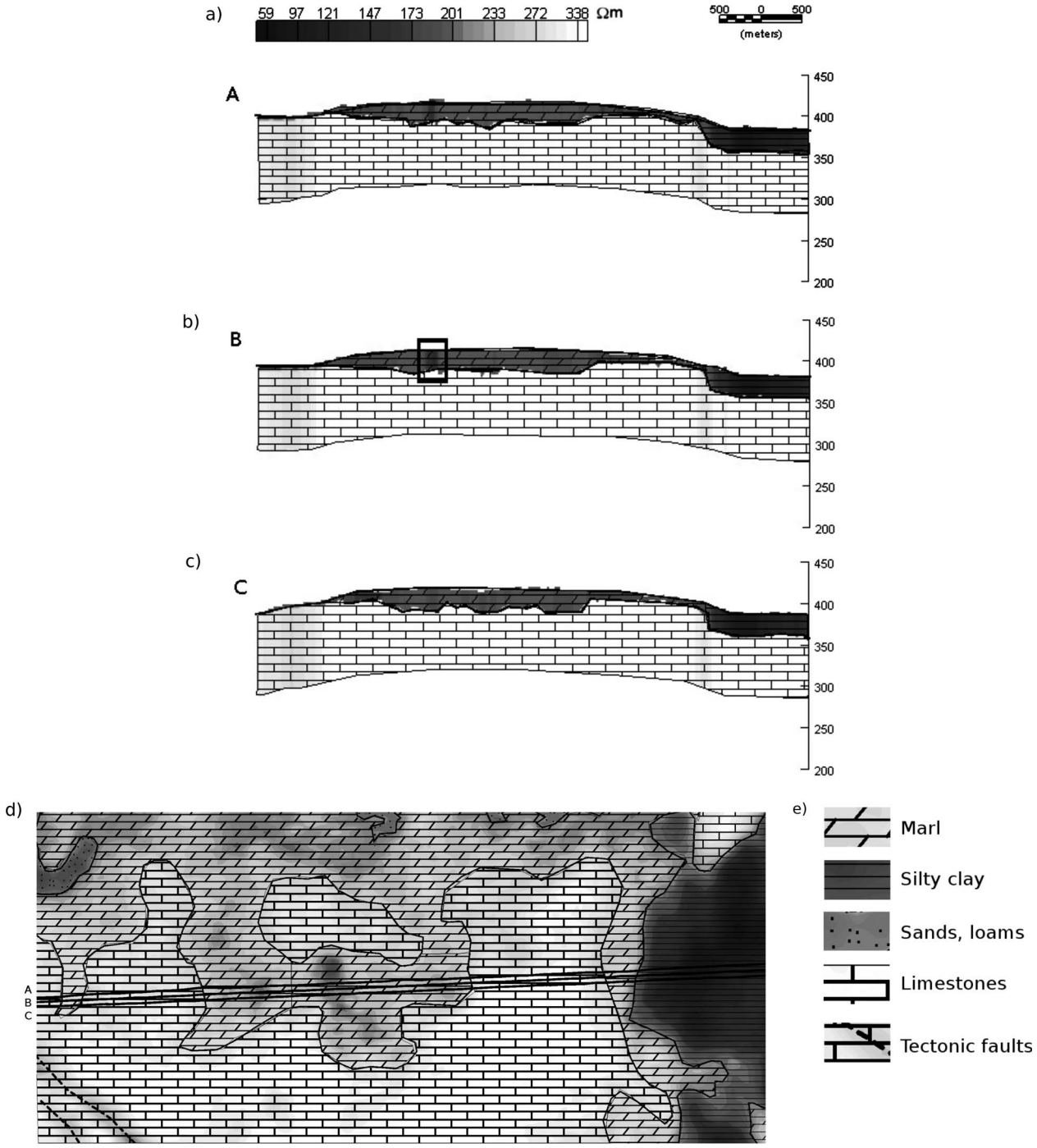

Figure 6. a) through c) 1D inversion results with a local anomaly associated with talik or karst marked in B; d) Resistivity map at effective depth of 30 m; e) legend. These sections characterize material composition of sediments of different ages. Each section's vertical axis is an absolute height in meters (Eastern Siberia data).

may be also interpreted as loose sediments with different genesis. In Fig. 11 the soil thickness is mapped on digital elevation model, and it gives more suggestions for interpretation. For example, zones of terrigenous material accumulation can be clearly seen as zones of increased thickness and interpreted as hydrodynamic traps in foothill regions. We can also mark areas of distribution of lateritic crusts on crystalline basement rocks and zones of increased thickness of alluvial sediments.

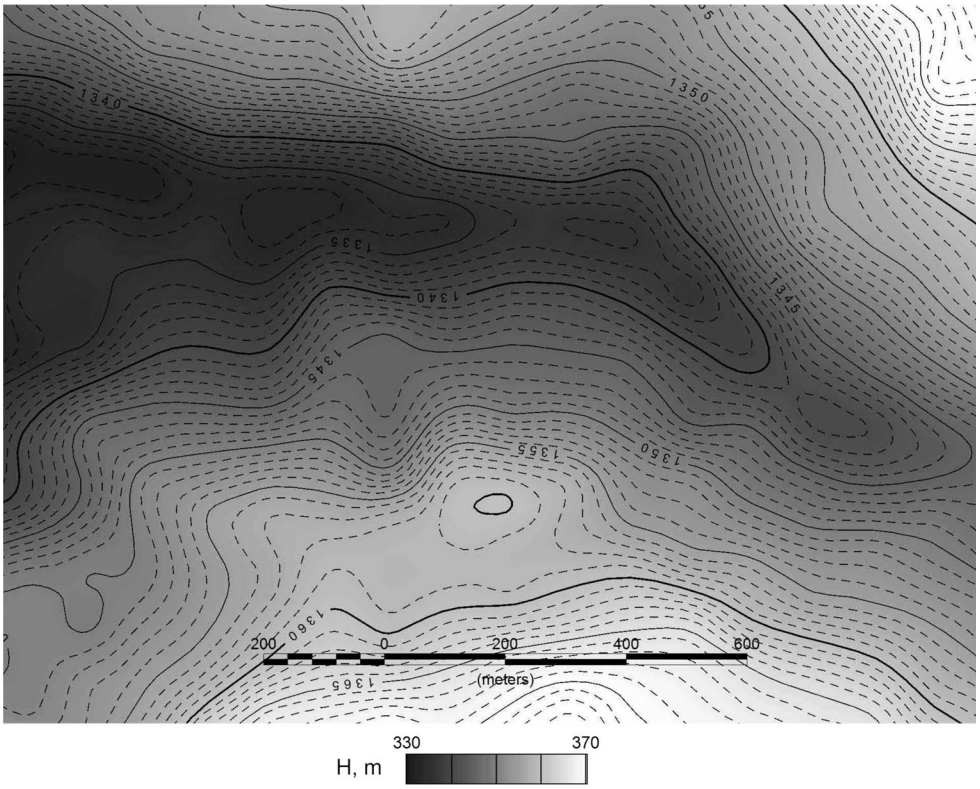

Figure 7. A fragment of digital elevation (H) map based on airborne geophysical data. Contour interval (between dotted lines) is 1 m.

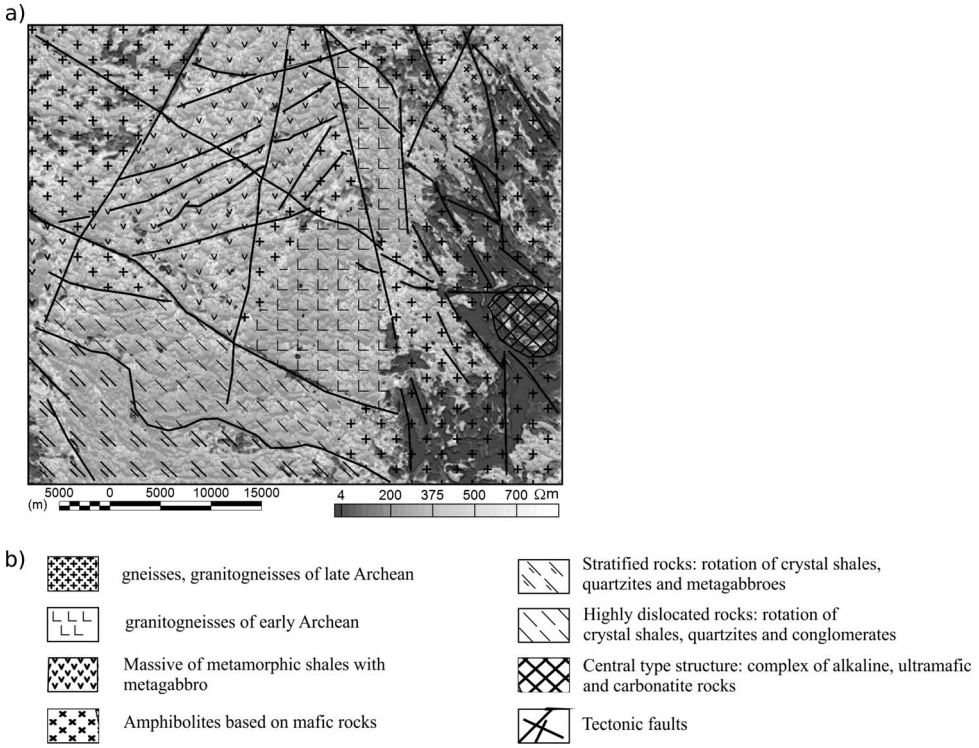

Figure 8. Mapping results of lithology-petrological characteristics of rocks on the Angolan shield: a) apparent resistivity map for effective depth of 20 m, color bar is in Ω·m; b) legend.

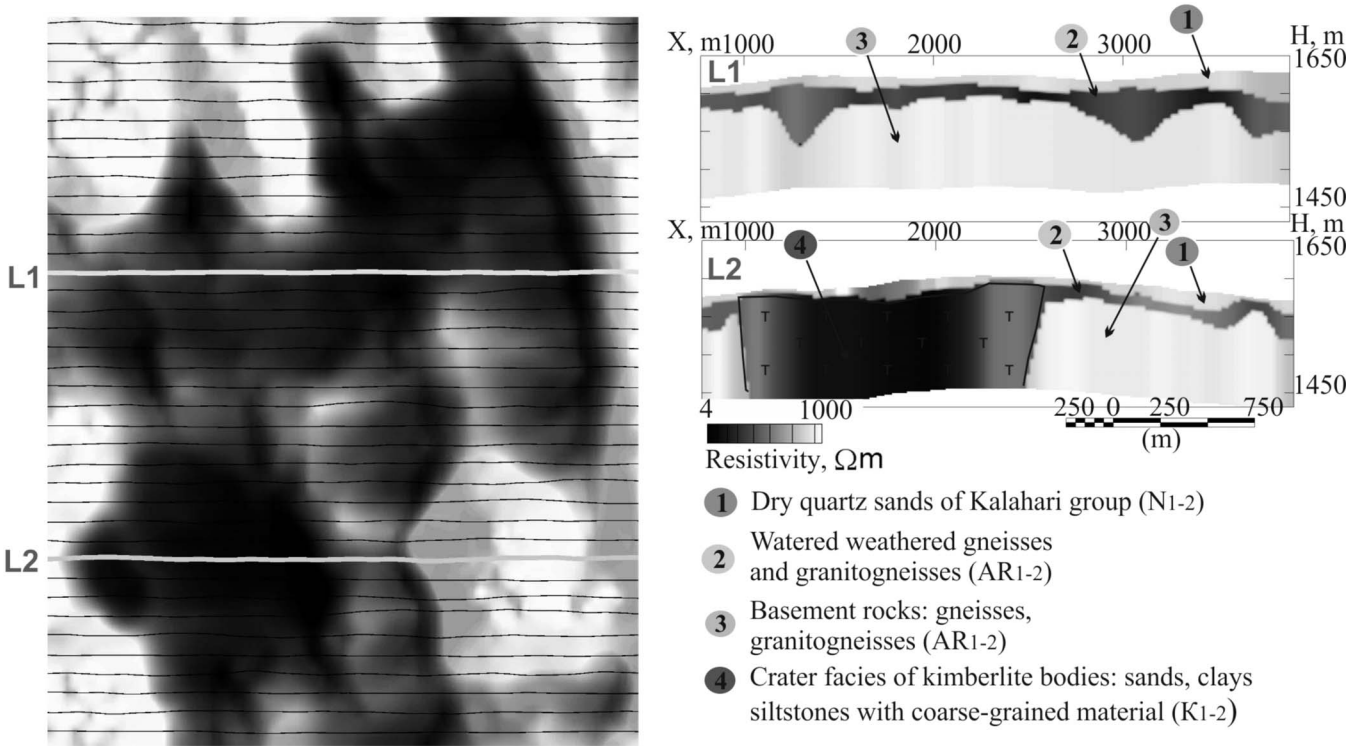

Figure 9. The example of analysis of thickness of layers that overlay the basement: apparent resistivity map for effective depth of 20 m and geoelectrical cross-sections from the result of 1D inversion. White lines on the map correspond to L1 and L2 sections with results on the right hand side. Vertical axes on the sections equate to absolute height H in meters, horizontal axes are the distances, X, in meters.

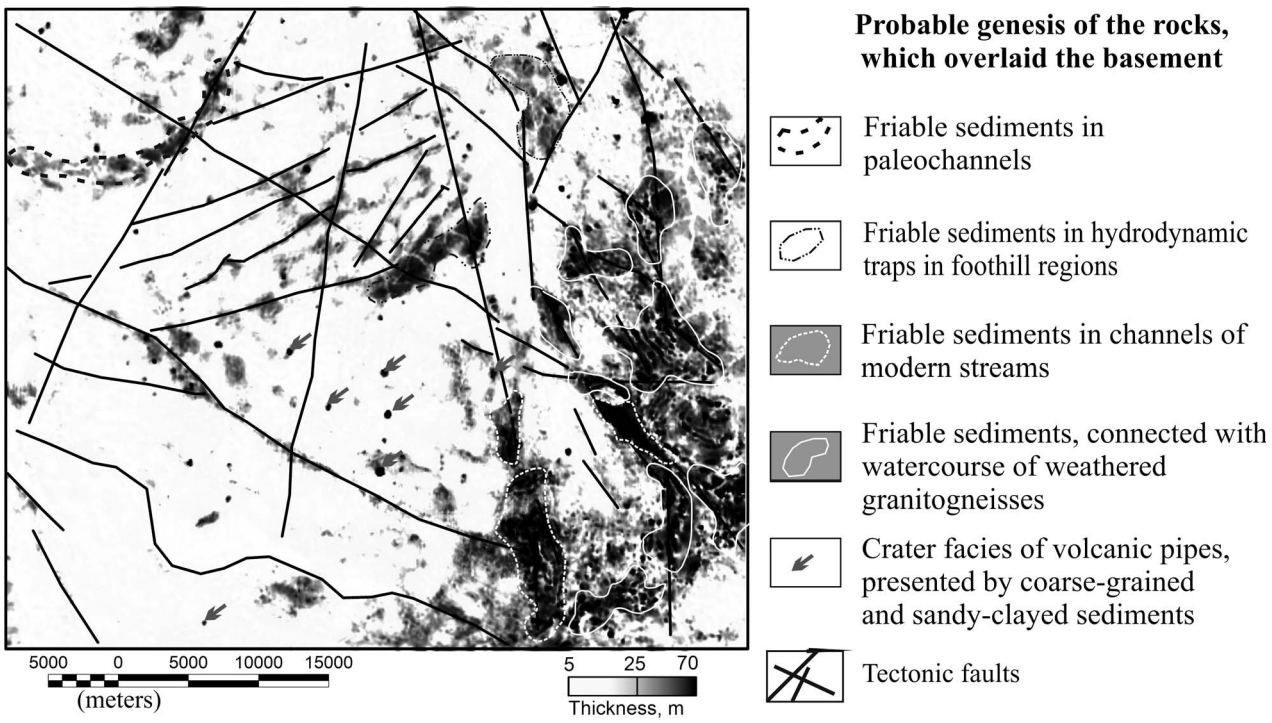

Figure 10. Sediments thickness map based on 1D inversion of airborne EM data. Major tectonic faults are shown as black lines.

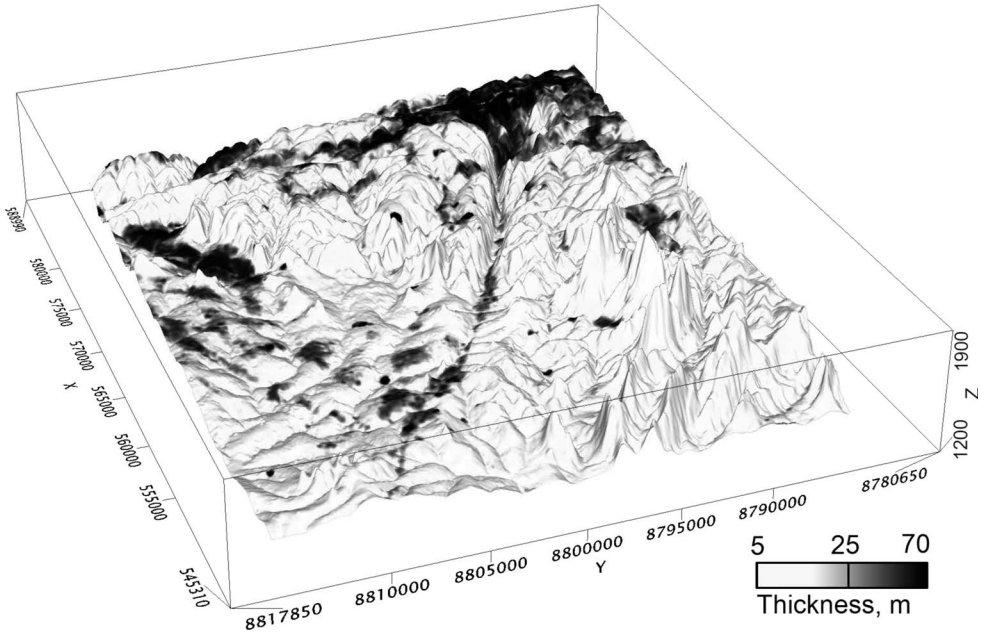

Figure 11. Soil thickness mapped on digital elevation model. Thickness was calculated as sum of first two layers in a three-layer inversion model. The third layer equates to an insulating basement.

Conclusions

We have demonstrated the capability of the EQUATOR system to provide EM data both in time and frequency domains, allowing extraction of maximum information about survey areas. In particular, we have demonstrated capabilities to recover electrical conductivity of the upper part of the cross-section. As a consequence, we allow a more accurate description of conductive anomalies. Further combination of electromagnetic, magnetic and altimeter data has led us to important conclusions about geological structures and tectonic features.

Therefore, we can confirm that a high-resolution airborne survey should be the initial part of investigation for many engineering and environmental tasks. Such surveys can reduce the volume of traditional ground based investigations (ground surveys, well drilling, laboratory testing). It optimizes total cost.

Acknowledgments

We wish to thank V. Kaminski, as well as all the reviewers, who put a good deal of effort into helping us improve this paper.

References

Becker, A., Barringer, A.R., and Annan, A.P., 1987, Airborne electromagnetics 1978–1988, *in* Developments and Application of Modern Airborne Electromagnetic Surveys, Fitterman, D.V., (ed.), United States Geological Survey Bulletin, **1925**, 9–20.

Collett, L.S., 1986, Development of the airborne electromagnetic techniques, *in* Airborne Resistivity Mapping, Palacky, G.J. (ed.): Geological Survey of Canada Paper, **86–22**, 9–18.

Felix, J.T., Karshakov, E.V., Melnikov, P.V., and Vanchugov, V.A., 2014, Data comparison results for airborne and ground electromagnetic systems used for kimberlites exploration in the Republic of Angola: Geophysika, **4**, 17–22 (in Russian).

Hinze, W.J., von Frese, R.R.B., and Saad, A.H., 2013, Gravity and magnetic exploration: Principles, practices and applications: Cambridge University Press, 512 pp.

Hodges, G., 2013, The power of frequency domain: When you should be using it: Extended Abstracts of the 6th International AEM Conference & Exhibition, 5 pp.

Kaminski, V., Viezzoli, A., and Menghini, A., 2015, Case studies of modeling IP effect in AEM data: Extended Abstracts of the Near Surface Geoscience Conference, 5 pp.

Karshakov, E., Volkovitsky, A., and Tkhorenko, M., 2013, Receiver positioning by means of EM field measurements: Extended Abstracts: 6th International AEM Conference & Exhibition, 4 pp.

Kaufman, A.A., 1989, A paradox in geoelectromagnetism, and its resolution, demonstrating the equivalence of frequency and transient domain methods: Geoexploration, **25**, 287–317.

Kozak, S.Z., Ageev, V.V., Moilanen, E.V., Karshakov, E.V., and Tkhorenko, M.Yu., 2015, Joint analysis of ground and airborne TEM surveys for groundwater exploration in difficult conditions of Yakutian region: Proceedings of Engineering Geophysics, 11th Research and Practice Conference & Exhibition, EAGE, 5 pp. (in Russian).

Lane, R., Plunkett, C., Price, A., Green, A., and Hu, Y., 1998, Streamed data—A source of insight and improvement for time domain airborne EM: Exploration Geophysics, **29**, 16–23.

Leick, A., Rapoport L., and Tatarnikov D., 2015, GPS satellite surveying, 4th ed.: John Wiley & Sons, New York, 840 pp.

Ley-Cooper, A., Macnae, J., and Viezzoli, A., 2010, Breaks in lithology: Interpretation problems when handling 2D structures with a 1D approximation: Geophysics, **75**, WA179–WA188.

Macnae, J., and Baron-Hay, S., 2010, Reprocessing strategy to obtain quantitative early time data from historic VTEM surveys: Proceedings of ASEG, 4 pp.

Moilanen, E., Karshakov, E., and Volkovitsky, A., 2013, Time domain helicopter EM system Equator: Resolution, sensitivity, universality: Extended Abstracts of the 6th International AEM Conference & Exhibition, 4 pp.

Pavlov, B.V., Volkovitskii, A.K., and Karshakov, E.V., 2010, Low frequency electromagnetic system of relative navigation and orientation: Gyroscopy and Navigation, **1**, 201–208.

Volkovitsky, A., and Karshakov E., 2013, Airborne EM systems variety: What is the difference? Extended Abstracts of the 6th International AEM Conference & Exhibition, 4 pp.

Zhdanov, M.S., 2009, Geophysical electromagnetic theory and methods: Elsevier, Amsterdam, 848 pp.